

VECTOR SLIDING MODE CONTROL OF SINUSOIDAL-FIELD SYNCHRONOUS SERVO DRIVE

István SCHMIDT, Katalin VINCZE and Károly VESZPRÉMI

Department of Electrical Machines and Drives
Budapest University of Technology and Economics
H-1521 Budapest, Hungary

Received: 17 Dec. 2001

Abstract

Permanent magnet synchronous servo drive with sinusoidal field is examined. The proposed control method is the sliding mode control, implementing the speed control, the current vector control, limitations and field weakening. The necessary sliding errors are derived. Different evaluation criteria are investigated by simulation and a new one is proposed. The combined vector sliding mode control, where the intervention depends on the magnitude of the sliding errors, is better than the traditional vector bang-bang control. The robustness of the bang-bang control is retained, the switching number and the steady state chattering are decreased.

Keywords: synchronous servo drive, sliding mode control, simulation, voltage vector selection.

1. Synchronous Servo Drive

The examined servo motor has a symmetrical three-phase stator and a permanent magnet rotor with sinusoidal spatial distribution of the flux density. Salient pole rotor is assumed without damping, so expressions $L_d \neq L_q$ and $L'_d = L_d, L''_q = L_q$ are valid for the synchronous and subtransient inductances respectively. For this case the equivalent circuits shown in *Fig. 1a,b,c* are valid. The permanent magnet is represented by a pole flux vector in the d direction with $\Psi_p = \text{const.}$ magnitude. Per-unit system is used for the calculations. The $d - q$ components, the $\bar{\psi} = \psi_d + j\psi_q$ flux vector and the $\bar{u} = R\bar{i} + d\bar{\psi}/dt + jw\bar{\psi}$ voltage vector are:

$$\psi_d = \Psi_p + L_d i_d, \quad \psi_q = L_q i_q, \quad (1)$$

$$u_d = R i_d + L_d di_d/dt - w L_q i_q, \quad u_q = R i_q + L_q di_q/dt + w L_d i_d + w \Psi_p. \quad (2)$$

It can be seen from the voltage equations, that the d component equation contains q quantity and the q component equation contains d quantity, i.e. there is a cross-coupling as well. Substituting the flux equations (1) to the torque equations:

$$m = \psi_d i_q - \psi_q i_d = \Psi_p i_q + L_{dq} i_d i_q, \quad (3)$$

where: $L_{dq} = L_d - L_q$.

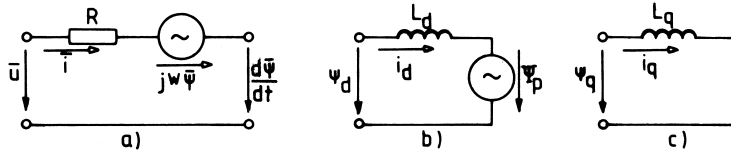


Fig. 1. Equivalent circuits of the sinusoidal-field synchronous servo motor

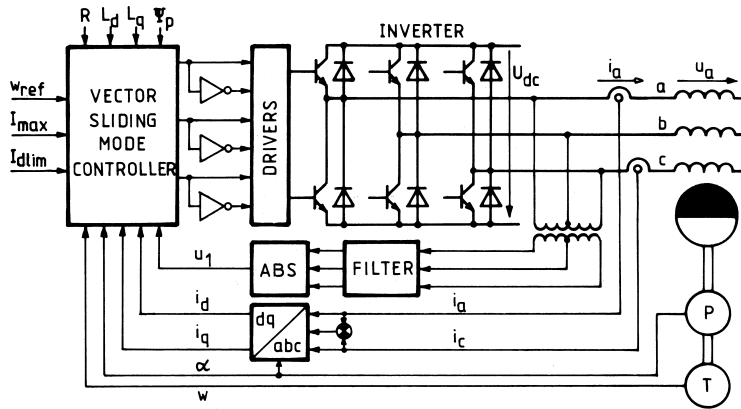


Fig. 2. The block diagram of the vector sliding mode control of the synchronous servo drive

The w angular speed and the α rotation angle are determined by the motion equations:

$$(m - m_\ell) / T_n = dw/dt, \quad w = d\alpha/dt, \quad (4)$$

where: $T_n = \theta W_n / M_n$ is the nominal starting time and m_ℓ is the load torque.

The synchronous servo motor is fed by a three-phase pulse width modulated (PWM) voltage source inverter. Using discrete time control, in every T_0 sampling instant the switching state of the inverter switches should be decided. The two level inverter in Fig. 2 is capable to switch $2^3 = 8$ kinds of voltage vectors to the motor terminals. It means seven different voltage vectors in stationary reference frame:

$$k = I \dots VI : \bar{u}_k = (2/3)U_{dc}e^{j(k-1)\pi/3}, \quad k = VII : \bar{u}_k = 0, \quad (5)$$

where: $U_{dc} = \text{const.}$ is the dc voltage of the inverter and the $\bar{u}_{VII} = 0$ can be developed in two ways.

The sliding mode digital control algorithm selects in every T_0 sampling instant directly (without any dedicated PWM modulator) the voltage vector best for the next T_0 interval.

The basic control task is the torque, speed or position control and the drive specific control task is the pole-field oriented current vector control. The operating regions and the limits of the $\bar{I}_1 = I_1 e^{j\vartheta_p} = I_{1d} + jI_{1q}$ fundamental current vector to be controlled are given in $d - q$ coordinate system fixed to the pole-flux in Fig.3 ϑ_p is the torque angle, I_n is the nominal, I_{\max} is the maximal motor current, $I_{d\lim}$ is the limit of the direct current. The following operating regions can be distinguished in the figure (motor and generator operation are related to $w > 0$ speed):

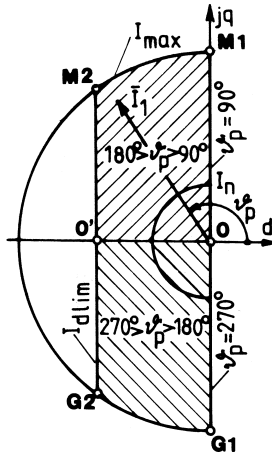


Fig. 3. Operation regions and limits in $d - q$ coordinate system

- Line 0-M1: simple normal motor operation ($I_{1d} = 0, \vartheta_p = 90^\circ$),
- Upper shaded region $I_{1q} > 0$: field weakening motor operation ($I_{d\lim} < I_{1d} < 0$),
- Line 0-G1: simple normal generator operation ($I_{1d} = 0, \vartheta_p = 270^\circ$),
- Lower shaded region $I_{1q} < 0$: field weakening generator operation ($I_{d\lim} < I_{1d} < 0$),
- Circle parts M1-M2 and G1-G2: current limit ($I_1 = I_{\max}$),
- Line M2-G2: limit of the direct current ($I_{1d} = I_{d\lim} \approx -\Psi_p/L_d$)
- Line 0-0': mechanical no-load ($I_{1q} = 0, \vartheta_p = 180^\circ$).

2. Sliding Mode Control

The sliding mode control is the generalization of the bang-bang control with such controlled quantities, where the differential equation of the control signal has order $n > 1$. The evaluating algorithm of the sliding mode control is based on the sliding error which has the same dimension as the control error $\Delta x = x_{\text{ref}} - x$:

$$s = \lambda_0 \Delta x + \lambda_1 d\Delta x/dt + \dots + \lambda_{n-1} d^{(n-1)} \Delta x/dt^{(n-1)}. \quad (6)$$

There are as many s_i sliding error signals in the algorithm as x_i quantities to be controlled. Having more s_i sliding errors they should be ranked in the algorithm. Having more variables with the same rank they are in co-ordinate relation if they should be controlled simultaneously. Co-ordination of the sliding errors is possible, if they can be controlled independently, i.e. for which the system is decoupled, or only weak cross-coupling exists in the control. In subordinated controls priority order of the evaluation of the sliding errors should be established.

In the case of synchronous servo drives the controller can operate with s_1, s_2, \dots, s_5 sliding errors. The s_1 performs one of the above mentioned basic control tasks while s_2 effects the current vector control. In a servo drive these two tasks are simultaneous, so s_1 and s_2 are in co-ordinated relation in the evaluation algorithm.

The s_1 sliding error for speed control is:

$$s_1 = \Delta w + \lambda d\Delta w/dt; \quad \Delta w = w_{\text{ref}} - w; \quad \lambda > 0, \quad (7)$$

where Δw is the speed error. If the basic task is the torque or position control, the s_1 sliding error should be defined in the following ways: for torque control: $s_1 = \Delta m$, $\Delta m = m_{\text{ref}} - m$, for position control:

$$s_1 = \Delta \alpha + \lambda_1 (d\Delta \alpha/dt) + \lambda_2 (d^2 \Delta \alpha/dt^2), \quad \Delta \alpha = \alpha_{\text{ref}} - \alpha.$$

The s_2 sliding error is used to control the direction of the current vector in the simple normal operation of the synchronous servo drive. In this operation the current vector must be synchronized by $\vartheta_p = \pm 90^\circ$ torque angle to the d direction determined by the rotor magnet. It means that the reference value of the stator current d component must be set to $i_{d\text{ref}}=0$. So the definition of the sliding error for the current vector direction in simple normal operation is:

$$s_2 = \Delta i_d = i_{d\text{ref}} - i_d, \quad \text{where } i_{d\text{ref}} = 0. \quad (8)$$

The basic sliding mode control algorithm of the normal operation (without current limit) of the speed controlled synchronous servo drive is based on the s_1 and s_2 sliding errors. The sign of s_1 and s_2 must be determined in every sampling instant and such a switching state must be set by the inverter by which the system satisfies the sliding conditions simultaneously:

$$s_1 \dot{s}_1 < 0 \quad \text{and} \quad s_2 \dot{s}_2 < 0. \quad (9)$$

To do this, the sign of \dot{s}_1 and \dot{s}_2 corresponding to all \bar{u}_k voltage vectors must be determined. The derivatives of the errors are:

$$\dot{s}_1 = ds_1/dt = d\Delta w/dt + \lambda d^2\Delta w/dt^2, \quad (10)$$

$$\dot{s}_2 = ds_2/dt = d\Delta i_d/dt. \quad (11)$$

For stepping w_{ref} speed reference at $t > 0$: $d\Delta w/dt = -dw/dt$, $d^2\Delta w/dt^2 = -d^2w/dt^2$, since $w_{\text{ref}} = \text{const}$. Since $i_{d\text{ref}} = 0$, $d\Delta i_d/dt = -di_d/dt$. So the signs of \dot{s}_1 and \dot{s}_2 are determined by the derivatives of the controlled quantities: dw/dt , d^2w/dt^2 and di_d/dt . These can be written using (2)–(4):

$$dw/dt = (\Psi_p i_q + L_{dq} i_d i_q - m_\ell)/T_n, \quad (12)$$

$$\frac{d^2w}{dt^2} = \frac{1}{T_n} \left[(\Psi_p + L_{dq} i_d) \frac{di_q}{dt} + L_{dq} i_q \frac{di_d}{dt} - \frac{dm_\ell}{dt} \right], \quad (13)$$

$$di_d/dt = (u_d - Ri_d + wL_q i_q)/L_d, \quad (14)$$

$$di_q/dt = (u_q - Ri_q - wL_d i_d - w\Psi_p)/L_q. \quad (15)$$

More simple results can be got by $L_d = L_q$, $L_{dq} = 0$ approximations:

$$\dot{s}_1 = -dw/dt - \lambda d^2w/dt^2 = -(\lambda\Psi_p/(T_n L_d))(u_q - u_{qo}), \quad (16)$$

where:

$$u_{qo} = -\frac{L_d}{\lambda} i_q + \frac{L_d}{\Psi_p \lambda} m_\ell + Ri_q + wL_d i_d + w\Psi_p + \frac{L_d}{\Psi_p} \frac{dm_\ell}{dt},$$

$$\dot{s}_2 = -di_d/dt = -(u_d - u_{do})/L_d, \quad (17)$$

where:

$$u_{do} = Ri_d - wL_d i_q.$$

The \dot{s}_1 and \dot{s}_2 sliding-error derivatives are determined by the inverter (motor) voltage vector $\bar{u} = u_d + ju_q$ and by the counter voltage vector $\bar{u}_o = u_{do} + ju_{qo}$ components. The u_{do} and u_{qo} counter voltages depend on the state variables of the drive. In steady-state apart from the current and torque pulsation: $m_\ell = m = \Psi_p i_q$ and $dm_\ell/dt = 0$, so:

$$u_{qo} = Ri_q + wL_d i_d + w\Psi_p, \quad u_{do} = Ri_d - wL_d i_q. \quad (18)$$

Shifting the axes by the instantaneous value of $\bar{u}_o = u_{do} + ju_{qo}$, the plane of the $d - q$ coordinate system can be divided to four parts (Fig. 4). For example, if a voltage vector pointing to the region **1** ($u_d > u_{do}$ and $u_q > u_{qo}$) is generated by the inverter, then $\dot{s}_1 < 0$ and $\dot{s}_2 < 0$ according to the above discussion. In this way the voltage vector pointing to the region **1** should be selected in the case when $s_1 > 0$ and $s_2 > 0$, since the conditions $s_1 \dot{s}_1 < 0$ and $s_2 \dot{s}_2 < 0$ are satisfied in this case. Region **2** must be selected, when $s_1 > 0$ and $s_2 < 0$, region **3** when $s_1 < 0$ and $s_2 < 0$ and region **4**, when $s_1 < 0$ and $s_2 > 0$.

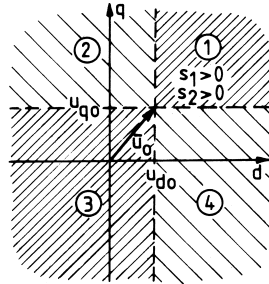


Fig. 4. The regions determining the selection of the voltage vector in $d - q$ coordinate system

The inverter can connect seven different \bar{u}_k voltage vectors to the motor terminals (5), forming a vector star in the $x - y$ stationary reference frame (Fig. 5). The $d - q$ coordinate system rotates with $w = d\alpha/dt$ angular speed in the $x - y$ coordinate system together with the rotor. To the regions 1...4 determined in the $d - q$ coordinate system, different voltage vectors can point depending on $\alpha(t)$ (Fig. 5). In the presented instant the selection of the voltage vector is unambiguous only in regions 1 and 2 (\bar{u}_{II} and \bar{u}_{III}). There are two vectors (\bar{u}_I and \bar{u}_{VI}) pointing to region 4, while there are three vectors (\bar{u}_{IV} , \bar{u}_V and \bar{u}_{VII}) satisfying the conditions of region 3. If there are more choices, one of them must be selected using a kind of criterion. For example, if the selection is done comparing the magnitude of the $s_1\dot{s}_1$ and $s_2\dot{s}_2$ products, then selecting the most negative or the least negative results in the most intensive or the most soft effect respectively.

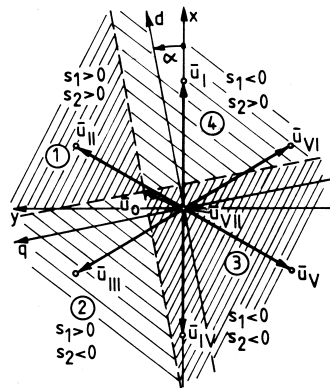


Fig. 5. Selection of the voltage vector in $x - y$ coordinate system

It is also possible that none of the \bar{u}_k vectors point to one of the regions. In this case without special treatment the sliding mode control stops. The boundary

case is shown in Fig. 6, when the \bar{u}_{II} and \bar{u}_{III} vectors point to the boundary of the region 1. Assuming large w speed, the approximating values of the (18) components are: $u_{qo} \approx w\Psi_p$, $u_{do} \approx 0$. By these in this boundary case: $\bar{u}_o = jw\Psi_p = j(2/3)U_{dc} \cos 60^\circ = jU_{dc}/3$. It means that at least $U_{dc\min} = 3w_{\max}\Psi_p$ inverter voltage is necessary not to stop the sliding mode control if there is no voltage vector in one of the regions. Considering the approximations, $U_{dc} \geq 4w_{\max}\Psi_p$ is necessary for safety's sake.

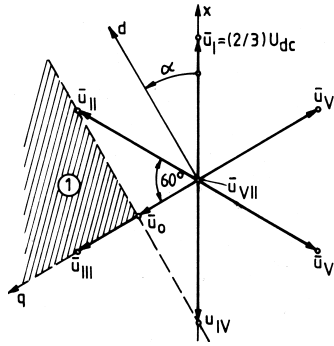


Fig. 6. Voltage vectors in boundary case

There are super-ordinated control tasks besides the basic ones based on the s_1 and s_2 signals. They can be performed by introducing the s_3 , s_4 , s_5 sliding errors to the algorithm.

The s_3 sliding error is used to limit the current and the torque. This modifies the intervention determined by s_1 and s_2 , if the magnitude of the \bar{i} current vector is greater than the allowed I_{\max} . The intervention modifies the above described deciding procedure as the sign of s_1 would be inverted. For example, if the speed control by s_1 sets too large accelerating torque causing over-current, then s_3 inverts the intervention in respect to u_q , i.e. decreases the i_q current component. It operates similarly in braking and in reverse rotation operation too. The definition of s_3 is:

$$s_3 = I_{\max} - \sqrt{i_d^2 + i_q^2}. \quad (19)$$

If $s_3 < 0$, then the above decision procedure must be evaluated as the sign of s_1 would have been reversed. It can be ensured e.g. by substituting s_1 in the (9) sliding condition by $s_1 = s_1 \text{sign}(s_3)$.

The s_4 sliding error is used to perform the field weakening operation. It operates only if the magnitude of the \bar{u}_1 terminal voltage vector formed from the u_{a1} , u_{b1} , u_{c1} fundamental (filtered) phase voltages of the motor exceeds a given U_{\max} value. It happens if the w_{ref} speed reference is so large that can be satisfied with $i_d = 0$ only by a voltage greater than U_{\max} . The intervention initiated by s_4 constraints an $i_d < 0$ field weakening current component ensuring $|\bar{u}_1| = U_{\max}$. It

overrides the effect of s_2 which performs $i_d = 0$ control in the normal operation mode. The definition of s_4 is:

$$s_4 = U_{\max} - |\bar{u}_1|. \quad (20)$$

If $s_4 < 0$, then such an intervention must be initiated which ensures the condition $di_d/dt < 0$, i.e. according to (17) $u_d < u_{do}$.

The s_5 sliding error is used to limit the i_d field weakening current component. It overrides the previous s_4 error signal, if the demagnetising i_d current component exceeds its limit $I_{d\lim}$ value. The definition of s_5 is:

$$s_5 = I_{d\lim} - i_d, \quad I_{d\lim} < 0. \quad (21)$$

If $s_5 > 0$, then such an intervention must be initiated which ensures the condition $\dot{s}_5 = -di_d/dt < 0$, i.e. $u_d > u_{do}$.

The above described control algorithm basically considers the s_1 and s_2 sliding error conditions to select the switching state of the inverter, but the conditions $s_3 < 0$, $s_4 < 0$ and $s_5 > 0$ override s_1 , s_2 and s_4 respectively.

3. Calculated Results

The permanent magnet synchronous machine is modelled by two electrical (14) (15) and two mechanical (12), (4) state equations. The sensors, the control circuits and the voltage source inverter are assumed to be ideal. The non-linear differential equation system is solved numerically by 4th order Runge-Kutta method. The calculated process is a speed controlled starting, normal operation with current limitation. In this way only the s_1 , s_2 and s_3 sliding errors are effective. The synchronous machine is considered to be cylindrical ($L_d = L_q$). The following parameters are used in per-unit system:

$$R = 0.04; \quad L_d = 0.4; \quad \Psi_p = 1; \quad U_{dc} = 5; \quad T_n = 0.1 \text{ s}; \\ W_n = 314/\text{s}; \quad I_{\max} = 3; \quad w_{\text{ref}} = 1.$$

The load torque is modelled by $m_\ell = m_{\ell o} + C_\ell w$. Instead of the t time, T_n nominal starting time and λ factor with dimension [s], the dimensionless $W_n t$, $W_n T_n$ and $W_n \lambda$ quantities are used. Demonstrating the simplicity of the examined sliding mode control only two control parameters can be varied: the T_0 sampling time and the λ factor. Their effect on the response of the drive to $u_{\text{ref}} = 1(t)$ speed reference step in the $0 \leq t \leq T = T_n$ time interval is presented in the following.

The larger the $f_0 = 1/T_0$ sampling frequency, the more easily the active sliding errors can be kept at zero value, so the more ideal the sliding mode control. Fig. 7 corresponds to the theoretical $f_0 = 200$ kHz sampling frequency. In Fig. 7a the characteristic time functions, in Fig. 7b the current vector are shown. It can be seen from the pulsation of the i_d and i_q current components and \bar{i} current vector

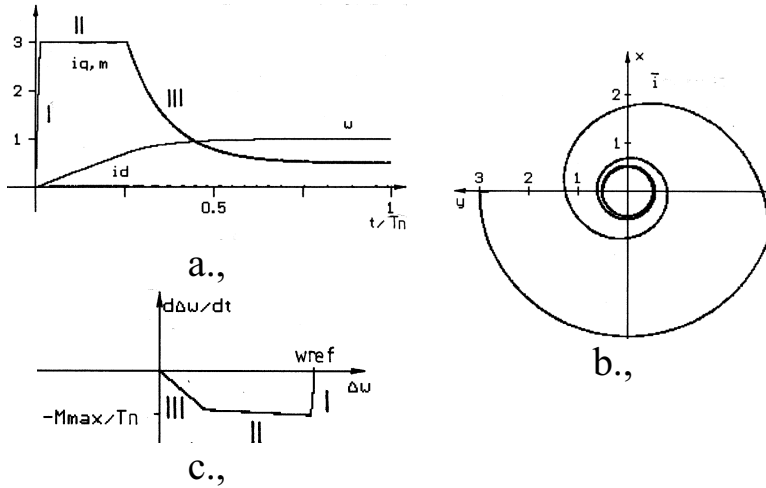


Fig. 7. Ideal sliding mode control ($f_0 = 200$ kHz; $m_\ell = 0.5 w$; $\lambda = T_n/9$, MAX case)

that this sampling frequency can be considered high. In the first section denoted by I, with $s_2 = -i_d \cong 0$ the i_q current component increases from 0 to I_{\max} . In the current limited section denoted by II $s_2 \cong 0$ and $s_3 \cong 0$, i.e. $i_q = I_{\max}$ and $m = M_{\max} = \Psi_p I_{\max}$. In the speed controlled section denoted by III $s_2 \cong 0$ and $s_1 \cong 0$, in the speed error phase plane (Fig. 7c) the drive moves towards the steady state (origin) on the sliding line with $\text{tg } \beta = -1/\lambda$ slope, while the time function of w speed approaches the w_{ref} reference exponentially with λ time constant (Fig. 7a). $\lambda = T_n/9$ is used to calculate Fig. 7.

The effect of the λ factor on the speed error phase plane is demonstrated in Fig. 8. The last section III of the speed setting on the sliding line with slope $\text{tg } \beta = -1/\lambda$ is independent of the load according to the robustness of the sliding mode control. The current limited section II is not always generated. If it is generated and the load torque is constant ($m_\ell = M_\ell = \text{const.}$), the acceleration and the derivative of the speed error are constant in this section. The magnitude of the latter is: $\Delta \dot{W}_o = (M_{\max} - M_\ell)/T_n$. Writing the λ factor in form $\lambda = T_n/(M_{\max} - M_\ell)/C$, if $C > 1$ there is a current limited section, if $C < 1$ there isn't. It can be proved considering the $\text{tg } \beta = \Delta \dot{W}_o/\Delta W_o$ slope that the transition is continuous from current limited operation to speed controlled operation at $\Delta W_o = (1 - M_\ell/M_{\max})/C$ speed error. It is clear from this consideration that the larger the load, the closer the speed to the w_{ref} reference value already at the end of the current limited operation.

The $f_0 = 200$ kHz sampling frequency is unfeasible practically, since the $T_0 = 1/f_0 = 5 \mu\text{s}$ is not enough to do the sampling and calculate the control algorithm. Furthermore, the resulting maximal switching frequency according to $f_{k \max} \leq 1/(2T_0) = f_0/2$ can be even 100 kHz, which is too high for the switches of the inverter. Using the nowadays available equipment (DSP based microcom-

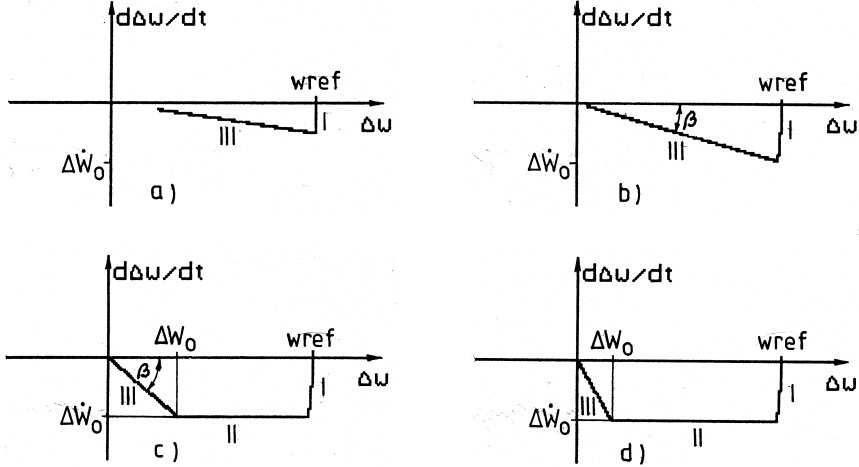


Fig. 8. Ideal sliding mode control on the speed error phase plane ($f_0 = 200$ kHz; $m_\ell = 0$; $\lambda = T_n/3/C$, MAX case). a. $C = 0.5$; b. $C = 1$; c. $C = 3$; d. $C = 6$

puter and IGBT inverter) the maximum for the feasible sampling frequency is $f_0 = 20$ kHz. This one is used to calculate Fig. 9 for the same quantities as in Fig. 7. Comparing the two figures it can be established, that there is a noticeable difference in the pulsation of the i_d and i_q current components, the \bar{i} current vector and the $m = \Psi_p i_q$ torque. The ± 0.1 pu pulsation is permissible, since the w speed as the main controlled signal is practically smooth, caused by the damping effect of the inertia of the mechanical system. It is not advisable to decrease the sampling frequency far below the $f_0 = 20$ kHz, since the pulsations are approximately inversely proportional to the f_0 frequency. Below a given f_0 , the torque pulsation would cause impermissible speed pulsation, and the current pulsation would generate significant additional losses.

If more voltage vectors satisfy the sliding conditions, those were selected so far (in Fig. 7–9), which provide

$$\max \left((u_d - u_{d0})^2 + (u_q - u_{q0})^2 \right). \quad (22)$$

This selection results in very intensive intervention and robust drive control. The robustness is got at the expense of high switching number. The switching numbers for the T simulation interval are shown in Table 1: k_0 is the number of the switchings resulting in $\bar{u}_k = 0$ voltage vector, k_1, k_2, k_3 are the number of single, double and triple switchings respectively, $k_v = k_1 + k_2 + k_3$ is the number of vector changing, $k_t = k_1 + 2k_2 + 3k_3$ is the number of transistor switchings. The data got according to (22) vector selection are in the MAX row of the Table. It can be established, that in this case the sliding controller never selects the $\bar{u}_k = 0$ voltage vector and the triple

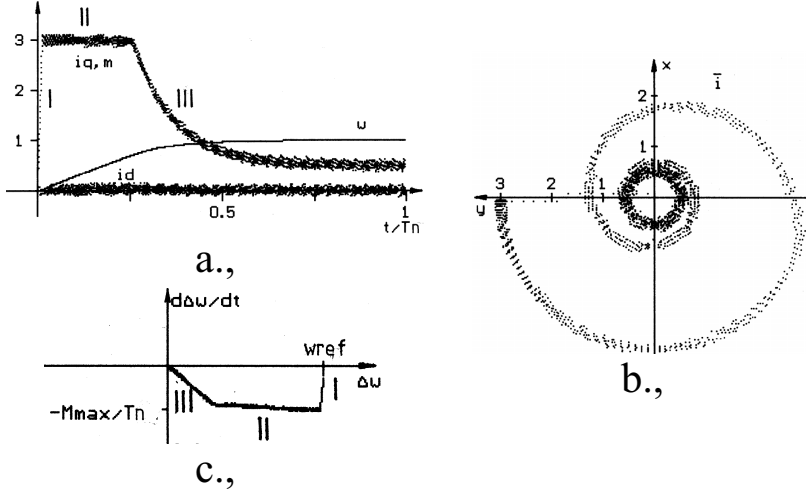


Fig. 9. Real sliding mode control ($f_0 = 20$ kHz; $m_\ell = 0.5$ w; $\lambda = T_n/9$, MAX case)

switching occurs very frequently, it is the so called vector bang-bang operation. According to this fact, the k_t/k_v average switching number for one vector changing is very high in this case. For an opposite selection criterion

$$\min ((u_d - u_{do})^2 + (u_q - u_{qo})^2), \quad (23)$$

the row MIN in Table 1 is got. As it can be seen, the sliding controller selects frequently $\bar{u}_k = 0$ voltage vector in this case, resulting in a significant decrease in the k_3 triple-, k_v vector changing- and k_t transistor switching numbers. However at the beginning of the transient starting process the development of the i_q current is slowed down as an effect of the many $\bar{u}_k = 0$ vectors in this case, the fast transient behaviour is lost (Fig. 10). Using the following combined selection criteria:

$$\begin{aligned} \min ((u_d - u_{do})^2 + (u_q - u_{qo})^2), & \quad \text{if } |s_1| < \varepsilon_1, \text{ or } |s_3| < \varepsilon_3, \\ \max ((u_d - u_{do})^2 + (u_q - u_{qo})^2) & \quad \text{else,} \end{aligned} \quad (24)$$

with properly selected ε_1 and ε_3 the robust operation can be retained and significant decrease in the switching number can be reached. The COMB row of Table 1 was calculated by using $\varepsilon_1 = \varepsilon_3 = 0.1$. Comparing with MAX row, significant decrease in the switching number can be reached in this case also. On the other hand the starting process in COMB case (Fig. 11) is practically the same as in the MAX case (Fig. 9), i.e. the fast reaching of the current limit is retained. Comparing Fig. 9 and 11 it can be established, that the lighter intervention in COMB case results in an approximately 50% decrease in the pulsation of the i_q current and the m torque in the section III and the next-coming steady state, comparing with the MAX case.

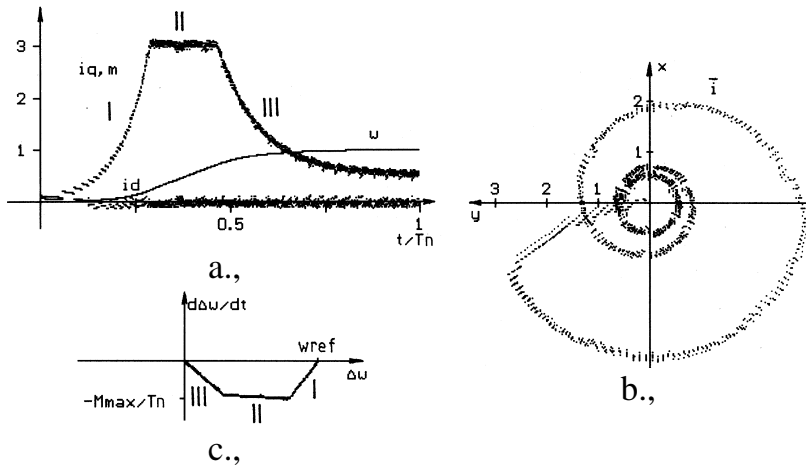


Fig. 10. Sliding mode control in MIN case ($f_0 = 20$ kHz; $m_\ell = 0.5$ w; $\lambda = T_n/9$)

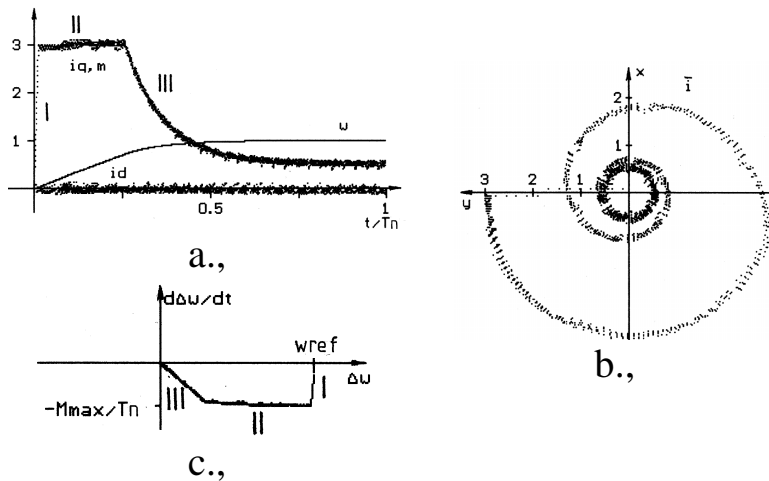


Fig. 11. Sliding mode control in COMB case ($f_0 = 20$ kHz; $m_\ell = 0.5$ w; $\lambda = T_n/9$)

The given k_v vector changing number could be maximum $Tf_0 = 2000$ for the T simulation time interval, if there is a vector changing in every sampling. In practice $k_v \leq Tf_0$, since it is not necessary to change the vector at every sampling.

The switching numbers in the next-coming also $T = T_n$ long steady state operation are given in Table 2. It can be seen, that the switching number in the COMB case is significantly less than in the MAX case here also, while the difference between the COMB and MIN cases is slight in this operation also.

Table 1.

CASE	k_0	k_1	k_2	k_3	k_v	k_t	k_t/k_v
MAX	0	300	790	784	1874	4232	2.26
MIN	395	756	425	74	1255	1828	1.46
COMB	482	959	513	116	1588	2333	1.47

Table 2.

CASE	k_0	k_1	k_2	k_3	k_v	k_t	k_t/k_v
MAX	0	376	750	783	1909	4225	2.21
MIN	531	1078	506	104	1688	2404	1.42
COMB	514	1101	488	107	1696	2291	1.35

4. Conclusion

The properties of the proposed combined vector sliding mode control, where the intervention depends on the magnitude of the sliding errors, are better than the traditional vector bang-bang control. The robustness of the bang-bang control is retained, the switching number and the steady state chattering are decreased.

Acknowledgement

This paper was supported by the Hungarian N.Sc. Found (OTKA No. T032207 and T030529) for which the authors express their sincere gratitude.

References

- [1] HASHIMOTO, H. – YAMAMOTO, H. – YANAGISAWA, S. – HARASHIMA, F., Brushless Servo Motor Control Using Variable Structure Approach. *IEEE Transactions on Industry Applications*, **24** No. 1. (1988), pp. 160–170.
- [2] SABANOVIC, A. – BILANOVIC, F., Sliding Mode Control of ac Drives. *IEEE Transactions on Industry Applications*, **25** No. 1. (1989), pp. 70–75.
- [3] MOERSCHELL, J., Digital Sliding Mode Torque Control for Induction Servo Drives. *IFAC. Motion Control of Intelligent Automation Conf. Perugia. Proc.*, (1992), pp. 277–282.
- [4] NAHDAM, P. K. – SEN, P. C., Accessible-States-Based Sliding Mode Control of Variable Speed Drive System. *IEEE Transactions on Industry Applications*, **31** No.4. (1995), pp. 737–743.
- [5] COMNAC, V. – CERNAT, M. – MOLDOVEANU, F. – CERNAT, R. M., Vector Control of Inverter-Fed Surface Permanent Magnet Synchronous Motors Using Sliding Mode. *EDPE'99. Int. Conf. Slovakia. Proc.*, (1999), pp. 262–267.
- [6] SCHMIDT, I. – VINCZE, K., – VESZPRÉMI, K., *Servo- and Robot Drives*, (in Hungarian). ISBN 963 420 642 5. Műegyetemi Kiadó. Budapest. p. 388. 2000.